Solubility measurement and correlation of 2-aminoterephthalic acid in eight alcoholic solvents at different temperatures

Eunhye Choi[a], Philippe M. Heynderickx[a,b,]*

[a] Center for Environmental and Energy Research (CEER) – Engineering of Materials via Catalysis and Characterization, Ghent University Global Campus, 119-5 Songdomunhwa-Ro, Yeonsu-Gu, Incheon, 406-840 South Korea; [b] Department of Green Chemistry and Technology, Faculty of Bioscience Engineering, Ghent University, 653 Coupure Links, Ghent, B-9000, Belgium; * Corresponding author: Philippe.Heynderickx@Ghent.ac.kr

Abstract

This research experimentally measured the solubility of 2-aminoterephthalic acid in eight pure alcoholic solvents – methanol, ethanol, 1-propanol, 1-butanol, 2-propanol, 2-butanol, 2-methyl-2-propanol, and 3-methyl-1-butanol – from 303.15 to 338.15 K at normal pressure p = 0.1 MPa by the excess solid method. The measured solubility of 2-aminoterephthalic acid in these pure organic solvents was found to increase with the rise of temperature in the following order: 3-methyl-1-butanol (lowest solubility) < 1-butanol < 2-butanol < 1-propanol < 2-methyl-2-propanol ≈ 2-propanol < ethanol < methanol (highest solubility). The experimental solubility was correlated by the Van't Hoff equation and the λh (Buchowski) equation. The apparent thermodynamic properties (Δ^0G_{sol}, Δ^0H_{sol} and Δ^0S_{sol}) were calculated by the Van't Hoff equation, from which it was concluded that the dissolution process is entropy-motivated and endothermal. In addition, the solvent effects on 2-aminoterephthalic acid solubility were studied by the KAT-LSER model, where the results showed that the polarizability accounts for 47.9 ± 4.2 % of the total solvent effect.

A volcano-type relation between the dissolution entropy and enthalpy versus the solvent boiling point is reported, showing maximal values of 55.3 J mol^{-1} K^{-1} and 29.2 kJ mol^{-1}, respectively, for intermediate molecular interactions of solute and solvent.

Keywords

2-aminoterephthalic acid, solubility, Van't Hoff equation, λh equation, solution thermodynamics, KAT-LSER model

1. Introduction

2-aminoterephthalic acid (Figure 1; IUPAC name: 2-amino-1,4-benzenedicarboxylic acid; molecular formula: $C_8H_7NO_4$; molecular mass: 181.15 g mol^{-1}; CAS number: 10312-55-7) is a significant pharmaceutical intermediate derived from terephthalic acid. It is also widely used as a linker for the construction of extended open frameworks such as IRMOF-3, amino-Zr-terephthalate MOF, NH_2-MIL-53(Al), and NH_2-UiO(Zr)-66 [1-3]. Its applicability in the functionalization of coordination polymers (CP) is attributed to its structural feature, where one amino group and two carboxyl groups are incorporated on its aromatic ring. The carboxylic groups on the ring build a coordination network by binding a center metal, whereas the amino group does not form any coordination, actively interacting with different solvents and triggering metal complex binding [4]. These free amino groups provide significant advantages to resulting amino-functionalized frameworks in terms of adsorption capacities and catalytic activities. One research group obtained Fe_3O_4@Ag-CP nanocomposites as a method for lead removal from water, employing the -NH_2 group as an adsorbent via synthesis of Fe_3O_4 and Ag-CP nanocomposites which were fabricated by $Ag(NO_3)$ and 2-aminoterephthalic acid dissolved in ethanol [5]. It is also reported that the coexistence of the amino group and hydroxyl group in the 2-aminoterephthalic acid structure provided exceptionally enhanced CO_2 affinity and selectivity to amino-functionalized metal organic framework (MOF) which are synthesized by solvothermal reactions in ethanol-DMF solution [4]. Its excellent performance as a basic catalyst can be found in molybdenum-zinc-based coordination polymers (Zn-Mo-ICP) which are produced by coordination-polymerization of 2-aminoterephthalic acid in hot methanol and zinc cation. The polymers exhibited superior conversion and selectivity in catalytic activity for olefin epoxidation via functionalization [6]. It is also verified that IRMOF-3 and NH_2-MIL-53(Al) coordinated by 2-aminoterephthalic acid acts as an excellent basic catalyst with high selectivity in the Knoevenagel condensation of ethyl cyanoacetate and ethyl acetoacetate with benzaldehyde [7].

Solubility is an essential physicochemical property that plays a significant role in the dissolution, crystallization, extraction, and purification process. Therefore, knowledge of the exact solubility is helpful for the optimization of industrial operating conditions and the design of the manufacturing process, where a specific compound is involved [8, 9]. However, despite the broad applications of 2-aminoterephthalic acid, no specific solubility data of 2-aminoterephthalic acid have been reported in the existing literature. Therefore, in the present study, the solubility of 2-aminoterephthalic acid in alcohol solvents (methanol, ethanol, 1-propanol, 1-butanol, 2-propanol, 2-butanol, 2-methyl-2-propanol, and 3-methyl-1-butanol) from 303.15 K to 338.15 K was experimentally determined using UV-VIS spectroscopy, and the correlation between the experimental solubility data and thermodynamic models was investigated.

2. Experimental part

2.1. Materials

Table 1 contains detailed information of the solute and solvents used, including CAS number, molecular formula, provenance (source), mass fraction purity and purification methods for 2-aminoterephthalic acid (solute) and the alcoholic solvents (methanol, ethanol, 1-propanol, 1-butanol, 2-propanol, 2-butanol, 2-methyl-2-propanol, and 3-methyl-1-butanol).

The solubility study of 2-aminoterephthalic acid in alcoholic solvents used a shaking thermostatic water bath (Hangil Biotech, Seoul, Korea) with precision of ± 0.1 K and a UV-VIS spectrophotometer (Optizen POP, Mecasys Co., Ltd, Korea).

2.2. Characterization methods

Powder X-ray diffraction (PXRD) was used to characterize the crystal structure of 2-aminoterephthalic acid before and after the solubility experiments. XRD patterns of the raw material and solids extracted from each solution were obtained by X-ray diffractometer Ultima IV (Rigaku, Japan) in Cu Kα radiation (40 kV and 40 mA). The 2θ-range was scanned from 3° to 100° using a step size of 0.02° at a scan rate of 8°/min. Crystal sizes are obtained via the Scherrer equation [10]. Prior to PXRD analysis of the undissolved solids, the samples were dried in a vacuum oven at 130°C for 2 hours at a pressure of 0.01 MPa.

The phase-transition temperature of 2-aminoterephthalic acid was experimentally obtained by a differential scanning calorimeter (DSC4000, Perkin Elmer) operated under a nitrogen atmosphere. The instrument calibration was carried out with lead (melting temperature = 600.6 K) as a reference material [11, 12]. Two samples of 2.41 mg and 4.71 mg of 2-aminoterephthalic acid was accurately placed in a sealed DSC pan, and the heat was continuously applied with a rate of 5 K min^{-1} from 298.2 to 650.2 K. The heat flows related to thermal transitions in the sample were investigated under a constant nitrogen gas flow with a rate of 15 mL min^{-1}.

Thermogravimetric analysis (TA instrument Q50) was used to indicate whether 2-ATA would decompose or not. In this work, 19.905 mg of 2-ATA was analyzed from 298.15 K to 648.15 K in an open pan under a nitrogen atmosphere with heating rate of 5 K min^{-1}.

2.3. Solubility measurements

The excess solid method was employed to acquire solid-liquid equilibrium between 2-aminoterephthalic acid and the used alcoholic solvents, and the solubility of the solute at equilibrium was determined using UV-VIS spectroscopy [13]. Experiments were carried out at atmospheric pressure (0.1 MPa) from 303.15 to 338.15 K.

First, an excess amount of 2-aminoterephthalic acid was dissolved in a single solvent to prepare a saturated solution. The tube containing the resulting solution was placed in a thermostatic bath and shaken at 160 rpm at the designated temperature for 20-24 hrs. The waiting time required to reach equilibrium was acquired from preliminary experiments. It was observed that after 20 hours, equilibrium was established, i.e., no significant change in solution concentration was observed. After equilibrium was established, a portion of liquid was carefully taken out from the saturated solution, using a syringe equipped with a PTFE syringe filter (0.22 μm) to exclude all suspended particles, and then transferred to another tube to appropriately dilute the solution with the corresponding solvent [14-16].

This solution was analyzed using a UV-VIS spectrophotometer to determine concentration in accordance with the calibration curve, see section S.1 in the Supplementary Content.

The molar fraction solubility, x_1, was obtained from Eq. (1), where m_i and M_i are the mass consumed and molar mass of the solute (subscript '1') and the solvent (subscript '2'), respectively:

$$x_1 = \frac{m_1/M_1}{m_1/M_1 + m_2/M_2} \tag{1}$$

Details can be found in section S.2 of the Supplementary Content. Solubility measurements were repeated at least three times for each data point to minimize experimental error.

Validation of the procedure was done by obtaining comparable solubility values for the known compound fumaric acid (IUPAC name: (2E)-but-2-enedioic acid; molecular formula: $C_4H_4O_4$; molecular mass: 116.072 g mol^{-1}; CAS number: 110-17-8) in ethanol in the temperature range 303-323 K. In addition, the presented experimental procedure to determine the solubility was also validated for the well-studied system benzoic acid (molecular formula: $C_7H_6O_2$; molecular mass: 122.123 g mol^{-1}; CAS number: 65-85-0) in water [17] and benzoic acid in ethanol [18-21].

Tabular data and graphical comparison between reported and experimentally obtained data for the aforementioned validation experiments are given in section S.3 of the Supplementary Content.

2.4. Modelling

2.4.1. Van't Hoff equation

The Van't Hoff equation is used to express the relationship between the solute's molar fraction solubility, x_1, and the temperature T (in K), see Eq. (2) [22-24]:

$$\ln x_1 = -\frac{\Delta H_{sol}}{RT} + \frac{\Delta S_{sol}}{R} \tag{2}$$

For simplicity, the solubility data are explicitly modeled using Eq. (3) with $A = \Delta S_{sol}/R$ and $B = -\Delta H_{sol}/R$:

$$x_1 = \exp\left(A + \frac{B}{T}\right) \tag{3}$$

The parameters A and B are obtained from the minimization of the objective function, given in Eq. (4), where index i refers to the experimental data:

$$S = \sum_{i=1}^{n} \left(x_{1,i,\mathrm{exp}} - x_{1,\mathrm{i,calc}}\right)^2 \xrightarrow[(A,B)]{} \min \tag{4}$$

Minimization of the objective function S is performed in Excel$^{®}$ with the GRG nonlinear method using forward derivatives and convergence at 10^{-4}. Standard deviations and confidence intervals for the parameters A and B are calculated according to standard procedures, see section S.4 in the Supplementary Content [25, 26].

It has to be noted that the well-known modified Apelblat equation [14, 15, 27-29], see Eq. (5), was also used to regress the experimental solubility data:

$$\ln x_1 = A + \frac{B}{T} + C \cdot \ln T \tag{5}$$

Based on the regression in this work, it appeared that the coefficient C could not be significantly estimated for all solvents, as the parameter value was always smaller than the corresponding confidence interval. In this respect, this parameter should be set equal to zero, see section S.4 in the Supplementary Content, and this automatically converts the modified Apelblat equation into the Van't Hoff relation.

2.4.2. λh equation

The λh equation was empirically formulated by Buchowski *et al.* [30, 31] to describe the solid-liquid phase equilibrium system, see Eq. (6). In this equation, two parameters, λ and h, are used to correlate the molar fraction solubility, x_1, and temperature T:

$$\ln\left(1+\lambda\frac{1-x_1}{x_1}\right)=\lambda h\left(\frac{1}{T}-\frac{1}{T_m}\right) \tag{6}$$

Solving Eq. (6) explicitly for the molar solubility results in Eq. (7):

$$x_1=\frac{\lambda}{\exp\left(\lambda h\left(\frac{1}{T}-\frac{1}{T_m}\right)\right)-(1-\lambda)} \tag{7}$$

The parameters λ and h represent the mean associated amount of solute molecules and the enthalpy of the solution, respectively [31]. These parameters are obtained from the minimization of the objective function, given in Eq. (8), where index i refers to the experimental data:

$$S=\sum_{i=1}^{n}\left(x_{1,i,\exp}-x_{1,\mathrm{i},\mathrm{calc}}\right)^2 \xrightarrow[(\lambda,h)]{} \min \tag{8}$$

Minimization of the objective function S is performed in Excel® with the GRG nonlinear method using forward derivatives and convergence at 10^{-4}. Standard deviations and confidence intervals for the parameters A and B are calculated according to standard procedures, see section S.4 in the Supplementary Content [25, 26].

3. Results and discussion

3.1. Experimental solubility of 2-aminoterephthalic acid in alcoholic solvents

The experimental and calculated solubility of 2-aminoterephthalic acid in methanol, ethanol, 1-propanol, 1-butanol, 2-propanol, 2-butanol, 2-methyl-2-propanol, and 3-methyl-1-butanol are plotted in Figure 2. The experimental solubility increases with increasing temperature and the increasing trend for solubility can be ranked according to the corresponding decreasing boiling point [32]: methanol (64.7°C, highest solubility) > ethanol (78.3°C) > 2-propanol (82.3°C) ≈ 2-methyl-2-propanol (82.4°C) > 1-propanol (97.2°C) > 2-butanol (99.6°C) > 1-butanol (117°C) > 3-methyl-1-butanol (131.2°C, lowest solubility).

As the solute 2-aminoterephthalic acid has three polar substituents (that is, two -COOH and one -NH_2), see Figure 1, the decreasing solubility according to the order methanol > ethanol > 1-propanol > 1-butanol > 3-methyl-1-butanol is explained by the increasing nonpolar carbon chain length. This is in accordance with earlier reports [33, 34].

An interesting observation is that the addition of one methyl group, comparing 2-propanol and 2-methyl-2-propanol, does not result in a significant difference in solubility, whereas 1-butanol and 3-methyl-1-butanol, differing in one methyl group positioned on C-3, display a factor of ~1.7 difference for the solubility of 2-aminoterephthalic acid. In the case of 1-propanol and 2-butanol, an intermediate factor of ~1.5 difference can be observed.

3.2. Powder X-ray diffraction analysis

All experimental samples involved in each solvent system, such as the raw 2-ATA compound and the excess undissolved solids in the suspension were characterized by the powder X-ray diffraction. The results for PXRD are mentioned in Figure 3a. Three peaks were observed with a P/N value (peak-to-noise) ratio, higher than 20%. They respectively occur at $2\theta = 15.16 \pm 0.04$, 27.22 ± 0.02 and 40.04 ± 0.04, see in Figure 3b. For these 2θ values, the crystal size was calculated using the Scherrer relation [10], and the results are shown in Figure 3c. It can be observed that the PXRD patterns of all the samples were almost identical. It illustrates that the crystal forms of all 2-ATA samples before and after the experiments were consistent. No other crystal forms were observed.

3.3. Melting thermodynamics

Details of the DSC measurements are given in section S.5 of the Supplementary Content. From this measurement the values for the melting temperature and melting enthalpy (and corresponding standard uncertainty) were apparently obtained as 319.67 ± 0.5 °C (592.82 ± 0.5 K) and 104.51 ± 2.16 kJ mol^{-1}, respectively. For the former value, the onset-temperature in the DSC analysis was considered [35, 36]. Typical values for a fusion enthalpy are between 5 kJ mol^{-1} and 80 kJ mol^{-1} [37], see Figure S-6 in the Supplementary Content and this observation might give a hint that the DSC data need to be revised and that the experimentally obtained values actually correspond to another process, rather than representing a melting temperature and the corresponding fusion enthalpy.

Inspection of the TGA result, see Figure S-9 in Supplementary Content, learns that ~100 K before the DSC peak there is already mass loss. At T = 319.67°C, there is a significant mass loss of 60%, so this cannot correspond to only a melting process; probably it comes with decomposition. Therefore, it can be concluded that this DSC analysis cannot be used to determine the melting point and the other thermodynamic properties of fusion. Since these thermodynamic data (melting point and fusion enthalpy) are important for correlating solubility data, they are estimated from correlations. It must be noted that the mass after the DSC analysis was not recorded and, hence, it could not be compared with the initial mass of the pan + sample, so no decisive information for possible mass losses during DSC could be obtained.

The model of Jain *et al.* [37, 38], combining the group additive and non-additive contributions to melting point, was used to estimate the T_m (K), $\Delta_{fus}H$ ($kJ\cdot mol^{-1}$) and $\Delta_{fus}S$ ($J\cdot K^{-1}\cdot mol^{-1}$) of 2-aminoterephthalic acid. This model has been used for estimating the melting point of over 2200 compounds, including certain structurally complex pharmaceutical compounds. The relevant expressions for this model are described by Eqs. (9) to (12), where the work of Dannenfelser *et al.* is referred to for the estimation of the fusion entropy [39]:

$$T_m = \frac{\Delta_{fus}H}{\Delta_{fus}S} \tag{9}$$

$$\Delta_{fus}H = \sum_i n_i m_i + \sum_j n_j m_j \tag{10}$$

$$\Delta_{fus}S = 50 - 8.314 \cdot \ln\sigma + 7.382 \cdot \tau \tag{11}$$

$$\tau = \mathrm{SP3} + \frac{1}{2}\cdot\mathrm{SP2} + \frac{1}{2}\cdot\mathrm{RING} - 1 \tag{12}$$

Using the values from Jain *et al.* [37], the fusion enthalpy is estimated as 31.15 kJ mol^{-1}. This value was compared to the value, obtained by the method of Keshavarz *et al.* [40], where a value of 31.62 kJ mol^{-1} was obtained. This corresponds nicely and based on the estimated values, the average value of 31.39 kJ mol^{-1} was taken for further calculations. For the calculation of the fusion entropy, $\Delta_{fus}H$, the value of 62.46 $J \cdot K^{-1} \cdot mol^{-1}$. Details are mentioned in section S.5 of the Supplementary Content. Based on Eq. (9) and the obtained estimates for fusion enthalpy and entropy, the melting temperature for 2-aminoterephthalic acid is estimated as 502.6 K (or 229.4°C).

From the DSC analysis results, it can be observed that around 225°C the endothermic peak starts. Given the estimated value for the melting temperature, it is believed that 2-ATA starts to melt around this temperature and that maybe new compounds are formed (linear or cyclic amides, as there are carboxylic acid groups and amino groups, which are known to form amide bonds), next to possible decomposition, as the mass loss is visible from the TGA analysis. These newly formed compounds (with bigger molar mass and typical strong interactions due to the hydrogen bonding, especially for primary amides) are probably the reason for the sharp peak around 319.67 ± 0.5 °C (592.82 ± 0.5 K) in the DSC result. Primary and secondary amides are known for their exceptional high boiling points and melting points [41]. Lastly, the gradual (slow) mass loss can be dedicated to the loss of water when amide bonds are formed. This observation was made by Zigansin *et al.* in their thermal analysis of the dipeptide L-isoleucyl-L-alanine, containing both amino and carboxylic acid groups [42] and these authors observed via mass spectrometric analysis that water (m/z = 18) and ammonia (m/z = 17) escaped from the sample, while it was heated. The first product clearly indicates amide formation, while the second corresponds to (partial) decomposition.

3.4. Solubility data correlation

The solubility of 2-aminoterephthalic acid is correlated by the Van't Hoff equation and λh equation. The calculated solubility values are listed in Table 2. The estimated parameters of A, B for the Van't Hoff equation are given in Table 3. Values for the parameters λ and h in the λh equation are listed in Table 4. In order to evaluate the accuracy of the solubility data and applicability of the kinetic models, the values for the root-mean square deviation (RMSD) and the average percentage relative deviation (APRD) are used. They are defined in Eqs. (13) and (14), respectively:

$$RMSD = \sqrt{\frac{1}{n} \cdot \sum_{i=1}^{n} \left(x_{1,i,\mathrm{exp}} - x_{1,\mathrm{i},\mathrm{calc}} \right)^2} \tag{13}$$

$$APRD = \frac{100}{n} \cdot \sum_{i=1}^{n} \frac{\left| x_{1,i,\mathrm{exp}} - x_{1,\mathrm{i},\mathrm{calc}} \right|}{x_{1,i,\mathrm{exp}}} \tag{14}$$

Both the RMSD and APRD values are listed in Tables 3 and 4. The maximal RMSD value is obtained for solvent 2-methyl-2-propanol and equals 3.77 10^{-4} mol mol^{-1} and 3.62 10^{-4} mol mol^{-1} for the Van't Hoff equation and the λh equation, respectively. The RAD value never exceeds 1.036 %. These results confirm that both thermodynamic models satisfactorily describe the experimental solubility data.

In order to determine which model best describes the data, a pooled residual sum of squares, see Eq. (15), is defined for the eight solvents used in this study via a simple arithmetic mean, with S_k obtained from Eqs. (4) and (8) for the Van't Hoff and Buchowski equation, respectively:

$$S_{pool} = \frac{1}{8} \cdot \sum_{k=1}^{8} S_k \qquad (15)$$

The value for S_{pool} equals 2.25 10^{-7} mol^2 mol^{-2} and 2.11 10^{-7} mol^2 mol^{-2} for the Van't Hoff and Buchowski equation, respectively. This means that the latter is the best to describe the global set of experimental data; however, the descriptive power of both models is quite comparable upon inspection of the results in Tables 3 and 4.

For the parameters A and B in the Van't Hoff equation, an interesting observation can be made. As these parameters correspond to $\Delta S_{sol}/R$ and $-\Delta H_{sol}/R$, respectively, the values for ΔS_{sol} and ΔH_{sol}, the so-called 'apparent thermodynamic properties' [33], can be calculated. It can be noted that the values for B are all negative and, hence, the values for ΔH_{sol} are all positive. This corresponds to the endothermic nature of the dissolution reaction (solubility increases as temperature increases). In other words, the addition of heat facilitates the dissolution reaction by providing energy to break bonds in the solid material. In Figure 4, values for ΔS_{sol} and ΔH_{sol} are plotted versus the corresponding boiling point of the used alcoholic solvents. The latter can be considered to be a measure for the non-polar part in the molecular structure (as they all have one hydroxyl group). Apparently, a polygonal line with two segments can fit these data, which indicates a specific relation between the solute and the used solvents, each of them having one hydroxyl group: for low boiling points, the dissolution enthalpy is increasing and from a certain point, a decreasing trend is observed. As the boiling point goes up, the non-polar part of the solvent increases and the polar groups in 2-aminoterephthalic acid experience an increasing repulsion, which gives rise to a higher required dissolution energy (enthalpy difference). However, as the solvent non-polar part gets bigger, the interaction with the non-polar aromatic ring can be considered to become the dominant interaction and the repulsion between polar and non-polar groups proportionally becomes smaller, resulting in a decrease of the dissolution enthalpy. In the whole process, the entropy difference becomes smaller upon better interaction, i.e., for lower and higher boiling points. This results in a maximal entropy difference at an intermediate boiling point value.

The two-segment line in Figure 4 is obtained via linear piece-wise regression (having seven parameters). The maximal enthalpy and entropy difference is equal to 29.2 kJ mol^{-1} and 55.3 J mol^{-1} K^{-1}, respectively, and it is obtained at $T^* = 381.1 \pm 2.4$ K. The entropy difference increases according to $(1.02 \pm 0.14)\cdot T_b$ for $T < T^*$ and decreases according to $(-2.18 \pm 0.39)\cdot T_b$ for $T > T^*$. For the enthalpy difference, the relations $(0.43 \pm 0.13)\cdot T_b$ and $(-0.64 \pm 0.26)\cdot T_b$ are found using confidence intervals with $t_{tab} = 2.685$ (details can be found in section S.6 in the Supplementary Content).

The observation in Figure 4 is reminiscent of the Sabatier principle in heterogeneous catalysis, where the interactions between the catalyst and the substrate should be neither too strong nor too weak – if the interaction is too weak, the molecule will fail to bind to the catalyst and no reaction will take place; on the other hand, if the interaction is too strong, the product fails to dissociate. For solubility, an inverse relation can be noted: for low solvent boiling points, the polar interactions dominate, whereas for high solvent boiling points, the non-polar interactions control the process. In between, neither interaction is weakly nor strongly present, giving rise to a maximal value for the dissolution enthalpy and entropy. A similar graphical representation is reported in the solubility of amiodarone HCl in mixtures of water and 1-methyl-2-pyrrolidone [43].

Next, a multiple linear regression analysis was implemented to investigate the effect of specific solvation interactions on the 2-aminoterephthalic acid dissolution process. The well-known KAT-LSER model, see Eq. (16), was used in this study [44]:

$$\ln x_1 = c_0 + c_1 \cdot \alpha + c_2 \cdot \beta + c_3 \cdot \pi^* + c_4 \cdot \frac{V_s \delta_H^2}{100RT} \tag{16}$$

The KAT-LSER model takes into account the contributions of hydrogen bond acidity (α), the hydrogen bonding basicity (β), the dipolarity/polarizability of investigated solvents (π*) and the remaining cavity term, including the Hildebrand parameter, δ_H, in total solvent effect. V_s is the solute molar volume, which was calculated as 116.998 cm^3 mol^{-1} at T = 298.15 K [45]. The values for α, β, and π* are listed in Table 5. Coefficient c_0 represents a constant for the model and depends only on the solute. Coefficients c_1 and c_4 are measures for the sensitivity of non-specific solute-solvent interaction and coefficients c_2 and c_3 are related to the influence of solute characteristics on the hydrogen bond of the solute-solvent system.

Application of the LINEST function in Excel® for multiple linear regression, see sections S.7 and S.8 in the Supplementary Content, shows that the parameters c_0 (the constant in the model) and c_4 cannot be significantly estimated (standard deviation > estimated parameter). This means that, for the given set of solvents, the hydrogen bond cohesion energy is not significant to describe the experimental solubility behavior. For the coefficients c_1, c_2 and c_3 significant values of -4.763 ± 0.850, -6.774 ± 0.540 and 10.60 ± 1.729 are found, respectively (n = 8, R^2 = 0.997, F = 654.7). The zero value of c_0 indicates that the cohesion of the crystal lattice does not significantly need energy to be overcome [46, 47]. The negative values for c_1 and c_2 indicate that the hydrogen bond donor and acceptor ability of the investigated solvents inhibit the solubility [48]. This is in line with the molecular structure of 2-aminoterephthalic acid, having two hydrogen donor groups (the carboxyl groups) and one hydrogen acceptor group (the amino group). The positive sign of π* suggests that the dipolarity/polarizability promotes the interaction between 2-aminoterephthalic acid and selected solvents [46-48]. The proportional contributions of α, β and π* to the overall solvent effect are 21.5 ± 4.9 %, 30.6 ± 4.2 % and 47.9 ± 4.2 %, respectively, where the polarizability takes the biggest share. Another noteworthy characteristic of the dissolution process is the specific contribution, ζ, of the enthalpy and entropy to the Gibbs energy. It is defined in Eqs. (17) and (18), with the harmonic mean temperature of the applied experimental temperature levels in this study, defined in Eq. (19) [33, 43, 49-51]:

$$\zeta_H = \frac{\left|\Delta^0 H_{sol}\right|}{\left|\Delta^0 H_{sol}\right| + \left|T_{hm}\,\Delta^0 S_{sol}\right|} \tag{17}$$

$$\zeta_{TS} = \frac{\left|T_{hm}\,\Delta^0 S_{sol}\right|}{\left|\Delta^0 H_{sol}\right| + \left|T_{hm}\,\Delta^0 S_{sol}\right|} \tag{18}$$

$$T_{hm} = n \cdot \left(\sum_{i=1}^{n} \frac{1}{T_i} \right)^{-1} \tag{19}$$

The values for $\Delta^0 H_{sol}$, $\Delta^0 S_{sol}$ and $\Delta^0 G_{sol}$, required in Eqs. (17) and (18), are obtained from a Van’t Hoff analysis, where the logarithm of the solubility versus the inverse of the temperature, corrected for the harmonic mean temperature, is plotted (with ξ the intercept in this plot), see Eqs. (20) to (22) [33, 51]:

$$\Delta^0 H_{sol} = -R \cdot \frac{\partial \ln x_1}{\partial\left(1/T - 1/T_{hm}\right)} \tag{20}$$

$$\Delta^0 G_{sol} = -RT_{hm} \cdot \xi \tag{21}$$

$$\Delta^0 S_{sol} = \frac{\Delta^0 H_{sol} - \Delta^0 G_{sol}}{T_{hm}} \tag{22}$$

For the presented calculations, it was assumed that the heat capacity of the solution can be considered constant according to the assumption that all thermodynamic values can be considered constant in a narrow temperature range [33].

The results for the thermodynamic parameters and the specific contribution to the Gibbs energy are shown in Table 6. The positive values for $\Delta^0 H_{sol}$ and $\Delta^0 S_{sol}$ indicate that the dissolution process is endothermic and entropy driven, as earlier obtained. When two solvents are compared, it can be observed that the lowest value for $\Delta^0 G_{sol}$ corresponds to the highest solubility, which is in accordance with general thermodynamic principles. All values of ζ_H are between 0.628 (2-butanol) and 0.911 (3-methyl-1-butanol), indicating energetic predominance on the dissolution process [51]. This corresponds with the findings of Garzón and Martínez [50], stating in their research that the main driving force of the ibuprofen dissolution process in organic solvents considered is the enthalpy, while for aqueous media the contributions are similar. Similar results are obtained by Li *et al.* for the dissolution of tinidazole in some (alcoholic) solvents [52].

Figure 5 shows a nice linear relation of the value for $\Delta^0 G_{sol}$ versus the boiling point of the used solvents. This corresponds well with the experimentally determined order of solubility and the conclusion of the KAT-LSER model, where the polarizability accounts for 47.9 ± 4.2 % in the dissolution process.

Finally, it can be verified that the Van't Hoff analysis, as given in section 2.4.1, gives similar values as given in this section. Since the analysis in section 2.4.1 is a nonlinear procedure and the Eqs. (20) to (22) are linear relations, slight differences are recorded for Δ^0S_{sol} and Δ^0H_{sol}, but they never exceed 1.8 % (for Δ^0S_{sol} with 1-butanol). Details and numerical values can be found in Supplementary Content section S.9.

4. Conclusions

The solubility of 2-aminoterephthalic acid in eight monohydroxy alcoholic solvents was experimentally measured in the temperature range 303.15 to 338.15 K at 0.1 MPa. The experimental solubility increases with increasing temperature and can be ranked as 3-methyl-1-butanol (lowest solubility) < 1-butanol < 2-butanol < 1-propanol < 2-methyl-2-propanol ≈ 2-propanol < ethanol < methanol (highest solubility). The solubility data were regressed by the Van't Hoff model and the Buchowski model. Upon comparing the complete set of experimental data, the latter model gives the best regression.

Apparent thermodynamic parameters of the dissolution process were obtained via a Van't Hoff analysis. This analysis shows that the main driving force of the 2-aminoterephthalic acid dissolution process is considered to be the enthalpy. The positive values for Δ^0H_{sol}, Δ^0S_{sol} and Δ^0G_{sol} show that the 2-aminoterephthalic acid dissolution process in the used alcoholic solvents is endothermic and entropy driven.

Specific solvent effects on the 2-aminoterephthalic acid dissolution process were studied by the KAT-LSER model, showing that the polarizability significantly accounts for 47.9 ± 4.2 % of the total solvent effect.

The dissolution entropy and enthalpy, ΔS_{sol} and ΔH_{sol}, versus the solvent boiling temperature can be modelled by a piece-wise linear model according to a volcano-type relation, clearly showing the molecular interactions between solute and solvent. This observation comes with a maximal dissolution enthalpy and entropy difference at 381.1 ± 2.4 K, equal to 29.2 kJ mol^{-1} and 55.3 J mol^{-1} K^{-1}, respectively.

Acknowledgements

E.C. acknowledges the Intensive Research Training Program of Ghent University Global Campus (GUGC), South Korea. E.C. and P.M.H. are thankful for the support from the Development Program of Ghent University Global Campus (GUGC), South Korea. The authors thank Prof. Jonathan Ozelton from the Center for Language and Learning (LLC) at Ghent University Global Campus (GUGC) for proofreading of the document. Dr. Els Bruneel (Department Of Chemistry, Faculty of Sciences, Ghent University) is thanked for the help with the analysis and interpretation of the DSC data. Dr. Keshab Adhikary (GUGC) is thanked for the help in the entropy of fusion calculation. The authors thank the reviewers for their constructive remarks.

List of Symbols

Roman symbols

A	coefficient in Eq. (3) (= $\Delta S_{sol}/R$) or Eq. (5)	-
B	coefficient in Eq. (3) (= $-\Delta H_{sol}/R$)	K^{-1}
B	coefficient in Eq. (5)	K
C	coefficient in Eq. (5)	-
h	coefficient in λh relation, see Eq. (6)	K
$\Delta_{fus}H$	fusion enthalpy	kJ mol^{-1}
ΔH_{sol}	solution enthalpy	kJ mol^{-1}
$m_{i\ or\ j}$	contribution of group i and proximity factor j to the $\Delta_{fus}H$	kJ mol^{-1}
n_i	number of occurrences [37]	-
n_j	proximity factor [37]	-
R	universal gas constant (8.3145)	J mol^{-1} K^{-1}
RING	number of independent single, fused, or conjugated aromatic ring systems	-
$\Delta_{fus}H$	fusion enthalpy	J mol^{-1} K^{-1}
$\Delta_{fus}S$	fusion entropy	J mol^{-1} K^{-1}
ΔS_{sol}	solution entropy	J mol^{-1} K^{-1}
S	residual sum of squares, defined in Eqs. (4) and (8)	mol^2 mol^{-2}
SP2	number of non-ring, non-terminal sp^2 atoms (=CH,=C,=N, C=O)	-
SP3	number of non-ring, non-terminal sp^3 atoms (CH_2, CH, C, NH, N, O, S)	-
T	temperature	K

T_{hm}	harmonic temperature, defined in Eq. (19)	K
T_m	melting temperature	K
x_1	molar fraction solubility, defined in Eq. (2)	mol mol^{-1}

Greek symbols

α	measure for hydrogen bond acidity [34], see Eq. (16)	-
β	measure for hydrogen bonding basicity [34], see Eq. (16)	-
δ_H	Hildebrand parameter, see Eq. (16)	$(J\ cm^{-3})^{1/2}$
ζ_X	contribution of X to the Gibbs energy, defined in Eqs. (17) and (18)	-
λ	coefficient in λh relation, see Eq. (6)	-
ξ	slope in the Van't Hoff plot [33]	-
π^*	measure for solvent dipolarity/polarizability [34], see Eq. (16)	-
σ	symmetry number	-
τ	flexibility number	-

Subscripts

1	solute
fus	fusion
H	enthalpy contribution, see Eq. (17)
hm	harmonic mean
pool	pooled value, see Eq. (15)
sol	solution
TS	entropy contribution, see Eq. (18)

Superscripts

0	calculated, according to the Van't Hoff analysis, see Eqs. (20) to (22)	

Abbreviations and acronyms

APRD	average percentage relative deviation, defined in Eq. (14)	%
CAS	Chemical Abstract Service (number)	-
CP	coordination polymer	
DMF	dimethylformamide	
DSC	differential scanning calorimetry	
GRG	generalized reduced gradient	
ICP	inductively coupled plasma	
IRMOF	isoreticular metal organic framework	
KAT	Kamlet, Abboud and Taft	
LSER	linear structure energy relation	
MIL	materials of Institute Lavoisier	
MOF	metal organic framework	
PTFE	polytetrafluoroethylene	
PXRD	powder X-ray diffraction	
rpm	rotations per minute	$\mathrm{min^{-1}}$
RAD	relative average deviation	$\mathrm{mol\ mol^{-1}}$
RMSD	root mean square deviation, defined in Eq. (13)	$\mathrm{mol\ mol^{-1}}$
TGA	thermogravimetric analysis	
UV-VIS	ultraviolet-visible light	

Reference list

[1] Q.Y. Yang, A.D. Wiersum, P.L. Llewellyn, V. Guillerm, C. Serred, G. Maurin, Functionalizing porous zirconium terephthalate UiO-66(Zr) for natural gas upgrading: a computational exploration, Chem. Comm. 47 (2011) 9603-9605.

[2] F. Xamena, F.G. Cirujano, A. Corma, An unexpected bifunctional acid base catalysis in IRMOF-3 for Knoevenagel condensation reactions, Micropor. Mesopor. Mat. 157 (2012) 112-117.

[3] S. Couck, J.F.M. Denayer, G.V. Baron, T. Remy, J. Gascon, F. Kapteijn, An amine-functionalized MIL-53 metal-organic framework with large separation power for CO_2 and CH_4, J. Am. Chem. Soc. 131 (2009) 6326-6327.

[4] Y. Yang, R.J. Lin, L. Ge, L. Hou, P. Bernhardt, T.E. Rufford, S.B. Wang, V. Rudolph, Y.Y. Wang, Z.H. Zhu, Synthesis and characterization of three amino-functionalized metal-organic frameworks based on the 2-aminoterephthalic ligand, Dalton T. 44 (2015) 8190-8197.

[5] A. Mehdinia, A. Mollazadeh-Moghaddam, A. Jabbari, Fabrication of silver-2-aminoterephthalic acid coordination polymer-coated Fe_3O_4 for effective removal of lead from aqueous media, Int. J. Environ. Res. 15 (2015) 631–644.

[6] M. Mohammadikish, S. Yarahmadi, Post modification of zinc based coordination polymer to prepare Zn-Mo-ICP nanoparticles as efficient self-supported catalyst for olefin epoxidation, Appl. Organomet. Chem. 33 (2019) e5052.

[7] J. Gascon, U. Aktay, M.D. Hernandez-Alonso, G.P. van Klink, F. Kapteijn, Amino-based metal-organic frameworks as stable, highly active basic catalysts, J. Catal. 261 (2009) 75-87.

[8] A. Noubigh, A. Mgaidi, M. Abderrabba, Solubility of gallic acid in liquid mixtures of (ethanol+ water) from (293.15 to 318.15) K, J. chem. Thermodyn. 55 (2012) 75-78.

[9] J. Wang, C. Xie, Q. Yin, L. Tao, J. Lv, Y. Wang, F. He, H. Hao, Measurement and correlation of solubility of cefmenoxime hydrochloride in pure solvents and binary solvent mixtures, J. chem. Thermodyn. 95 (2016) 63-71.

[10] P. Scherrer, Bestimmung der Gröβe und der inneren Struktur von Kolloidteilchen mittels Röntgenstrahlen,, Nachr. Ges. Wiss. Gttingen, Math.-Phys. Kl. 2 (1918) 98-100.

[11] https://webbook.nist.gov/cgi/inchi?ID=C7439921, consulted on August 11, 2022.

[12] G.D. Gatta, M.J. Richardson, S.M. Sarge, S. Stølen, Standards, calibration, and guidelines in microcalorimetry. Part 2. Calibration standards for differential scanning calorimetry, Pure Appl. Chem. 78 (2006) 1455-1476.

[13] S. Black, L.P. Dang, C.J. Liu, H.Y. Wei, On the measurement of solubility, Org. Process Res. Dev. 17 (2013) 486–492.

[14] H. Zhang, Q. Yin, Z. Liu, J. Gong, Y. Bao, M. Zhang, H. Hao, B. Hou, C. Xie, Measurement and correlation of solubility of dodecanedioic acid in different pure solvents from T=(288.15 to 323.15) K, J. chem. Thermodyn. 68 (2014) 270-274.

[15] G.B. Yao, Z.X. Xia, Z.H. Li, Thermodynamic study of solubility for 2-amino-4-chloro-6-methoxypyrimidine in twelve organic solvents at temperatures from 273.15 K to 323.15 K, J. chem. Thermodyn. 105 (2017) 187-197.

[16] Z. Han, H. Hao, H. Wu, Q. Liu, S. Zong, X. Huang, Solubility and thermodynamic properties of dirithromycin form A and form B in pure solvents and binary solvent mixture, J. chem. Thermodyn. 132 (2019) 240-249.

[17] https://trc.nist.gov/reference-systems/, consulted on August 12, 2022.

[18] A. Kumari, S. Kadakanchi, R. Tangirala, P.K. Thella, B. Satyavathi, Measurement and modeling of solid−liquid equilibrium of para-tert-butylbenzoic acid in acetic acid/methanol + water and acetic acid + para-tert-butyltoluene binary systems at various temperatures, J. Chem. Eng. Data 62 (2010) 87-95.

[19] J. Thati, F.L. Nordström, Å.C. Rasmuson, Solubility of benzoic acid in pure solvents and binary mixtures, J. Chem. Eng. Data 55 (2010) 5124-5127.

[20] R. Li, S. Zhan, G. Chen, Y. Jin, B. Yu, J. Zhao, D. Han, H. Fan, Equilibrium solubility, model correlation, and solvent effect of indole-3-acetic acid in twelve pure solvents, J. Chem. Eng. Data 64 (2019) 1802-1808.

[21] G. Zhao, Z. Deng, W. Yang, F. Li, Y. Song, X. Zhao, H. Sheng, Y. Hu, Solubility and thermodynamic parameters of 5-fluoro-2-oxindole in nine pure solvents and binary solventmixtures at T=(278.15–323.15) K, J. Mol. Liq. 298 (2019) 112015.

[22] F. Shakeel, M.F. Alajmi, N. Haq, N.A. Siddiqui, P. Alam, A.J. Al-Rehaily, Solubility and thermodynamic function of a bioactive compound bergenin in various pharmaceutically acceptable neat solvents at different temperatures, J. chem. Thermodyn. 101 (2016) 19-24.

[23] F. Shakeel, N. Haq, N.A. Siddiqui, Solubility and thermodynamic function of vanillin in ten different environmentally benign solvents, Food Chem. 180 (2015) 244-248.

[24] J. Ouyang, J. Wang, H. Hao, X. Huang, Y. Gao, Y. Bao, Y. Wang, Q. Yin, Determination and correlation of solubility and solution thermodynamics of valnemulin hydrogen tartrate in different pure solvents, Fluid. Phase Equilibr. 372 (2014) 7-14.

[25] R. de Levie, Estimating parameter precision in nonlinear least squares with Excel's solver, J. Chem. Educ. 76 (1999) 1594-1598.

[26] G.F. Froment, L.H. Hosten, Catalytic Kinetics: Modelling, in: J.R. Anderson, M. Boudart (Eds.) Catal.-Sci. Tech. , Springer-Verlag, Berlin, 1981, pp. 97-170.

[27] A. Apelblat, E. Manzurola, Solubility of oxalic, malonic, succinic, adipic, maleic, malic, citric, and tartaric acids in water from 278.15 to 338.15 K, J. chem. Thermodyn. 19 (1987) 317-320.

[28] A. Apelblat, E. Manzurola, Solubilities ofo-acetylsalicylic, 4-aminosalicylic, 3,5-dinitrosalicylic, andp-toluic acid, and magnesium-DL-aspartate in water from T=(278 to 348) K, J. chem. Thermodyn. 31 (1999) 85-91.

[29] Z. Yang, D. Shao, G. Zhou, Solubility measurement and thermodynamic model correlation of sancycline in 12 pure solvents, J. Chem. Eng. Data 64 (2019) 5665-5670.

[30] H. Buchowski, J.J. Kosinski, A. Ksiazczak, Activity of solvent and solubility, J. Phys. Chem. 92 (1988) 6104-6107.

[31] H. Buchowski, A. Ksiazczak, S. Pietrzyk, Solvent activity along a saturation line and solubility of hydrogen-bonding solids, J. Phys. Chem. 84 (1980) 975-979.

[32] F. Liu, C. Cao, B. Cheng, A quantitative structure-property relationship (QSPR) study of aliphatic alcohols by the method of dividing the molecular structure into substructure, Int. J. Mol. Sci. 12 (2011) 2448-2462.

[33] R. Cao, R. Zhang, X. Hu, J. Sha, G. Jiang, Y. Li, T. Li, B. Ren, Thermodynamic modelling, Hansen solubility parameter and solvent effect of oxaprozin in thirteen pure solvents at different temperatures, J. chem. Thermodyn. 151 (2020) 106239.

[34] Y. Marcus, The properties of organic liquids that are relevant to their use as solvating solvents, Chem. Soc. Rev. 22 (1993) 409-416.

[35] W. Hemminger, A review of the work of the German Society for Thermal Analysis (GEFTA) on standardization, J. Thermal. Anal. 40 (1993) 1437-1440.

[36] T. Lever, P. Haines, J. Rouquerol, E.L. Charsley, P. Van Eckeren, D.J. Burlett, ICTAC nomenclature of thermal analysis (IUPAC Recommendations 2014), Pure Appl. Chem. 86 (2014) 545-553.

[37] A. Jain, S.H. Yalkowsky, Estimation of melting points of organic compounds II, J. Pharm. Sci. 95 (2006) 2562-2618.

[38] A. Jain, G. Yang, S.H. Yalkowsky, Estimation of melting points of organic compounds, Ind. Eng. Chem. Res. 43 (2004) 7618-7621.

[39] R. Dannenfelser, S.H. Yalkowsky, Estimation of entropy of melting from molecular structure: A no-group contribution model, Ind. Eng. Chem. Res. 35 (1996) 1483-1486.

[40] M.H. Keshavarz, A.R. Akbarzadeh, R. Rahimi, M. Jafari, M. Pasandideh, R. Sadeghi, A reliable method for prediction of enthalpy of fusion in energetic materials using their molecular structures, Fluid. Phase Equilibr. 427 (2016) 46-55.

[41] D.J. Hart, C.M. Hadad, L. Craine, H. Hart, Organic Chemistry: A Short Course, 13th ed., Brooks Cole, Belmont, USA, 2011.

[42] M.A. Zigansin, R.A. Larionov, A.V. Gerasimov, S.A. Ziganshina, A.E. Klimovitskii, K.R. JKhayarov, T.A. Mukhametzyanov, V.V. Borbatchuk, Thermally induced cyclization of L-isoleucyl-L-alanine in solid state: Effect of dipeptide structure on reaction temperature and self-assembly, J. Pep. Sci. 25 (2019) e3177.

[43] S.H. Eghrary, R. Zarghami, F. Martínez, A. Jouyban, Solubility of 2-butyl-3-benzofuranyl 4-(2-(diethylamino)ethoxy)-3,5-diiodophenyl ketone hydrochloride (amiodarone HCl) in ethanol + water and N-methyl-2-pyrrolidone + water mixtures at various temperatures, J. Chem. Eng. Data 57 (2012) 1544-1550.

[44] M.J. Kamlet, J.L.M. Abboud, R.W. Taft, An examination of linear solvation energy relationships, Prog. Phys. Org. Chem. 13 (1981) 485-630.

[45] E.C. Ihmels, J. Gmehling, Extension and revision of the group contribution method GCVOL for the prediction of pure compound liquid densities, Ind. Eng. Chem. Res. 42 (2003) 408-412.

[46] H. He, J. Sha, Y. Wan, R. Sun, G. Jiang, Y. Li, T. Li, B. Ren, Solid-liquid phase equilibrium of naphazoline hydrochloride in eleven neat solvents: Determination, solvent effect, molecular simulation and thermodynamic analysis, J. Mol. Liq. 325 (2021) 114748.

[47] C. Li, J. Li, D. Wu, L. Qi, L. Zhou, C. Xie, J. Gong, W. Chen, Measurement and correlation of the solubility of kojic acid inpure and binary solvents, J. chem. Thermodyn. 167 (2022) 106712.

[48] R. Wang, C. Chen, W. Yang, P. Zhou, F. Zhu, H. Xu, G. Hu, W. Sun, W. Shen, Y. Hu, Solubility determination and thermodynamic characterization of orotic acid in twelve pure solvents and four binary mixed solvents, J. Mol. Liq. 341 (2021) 117335.

[49] Y. Guo, Y. Hao, Y. Zhou, Z. Han, C. Xie, W. Su, H. Hao, Solubility and thermodynamic properties of vanillyl alcohol in some pure solvents, J. chem. Thermodyn. 106 (2017) 276-284.

[50] L.C. Garzón, F. Martínez, Temperature dependence of solubility for ibuprofen in some organic and aqueous solvents, J. Solution Chem. 33 (2004) 1379-1395.

[51] D.R. Delgado, F. Martínez, Solubility and solution thermodynamics of sulfamerazine and sulfamethazine in some ethanol + water mixtures, Fluid. Phase Equilibr. 360 (2013) 88-96.

[52] T. Li, L. Zhu, J. Li, Z. Cao, J. Sha, Y. Li, B. Ren, Solubility, thermodynamic properties and molecular simulation of tinidazole in fourteen mono-solvents at different temperatures, J. chem. Thermodyn. 170 (2022) 106767.

[53] https://www.weather.go.kr/weather/observation/aws_table_popup.jsp, consulted on July 1, 2022.

[54] R.F. Fedors, A method for estimating both the solubility parameters and molar volumes of liquids, Polym. Eng. Sci. 14 (1974) 147-154.

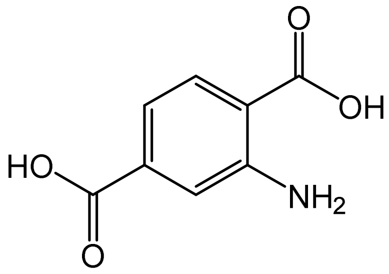

Figure 1: Molecular structure of 2-aminoterephthalic acid (2-amino-1,4-benzenedicarboxylic acid).

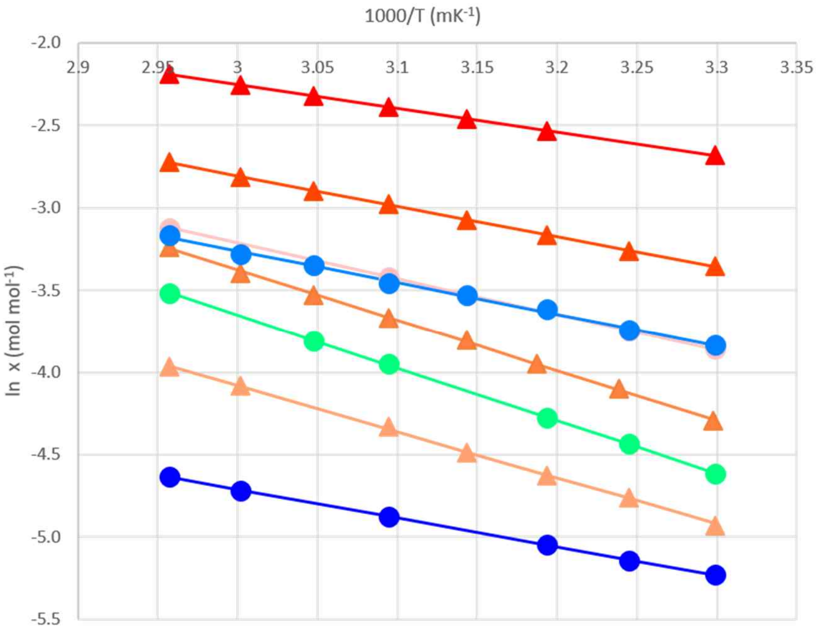

Figure 2: Logarithm of the molar fractional solubility of 2-aminoterphthalic acid in 8 alcoholic solvents versus temperature: (▲) methanol; (▲) ethanol; (▲) 1-propanol; (▲) 1-butanol; (●) 2-propanol; (●) 2-methyl-2-propanol; (●) 2-butanol; (●) 3-methyl-1-butanol; full lines are calculated with Eq. (2) (linear form).

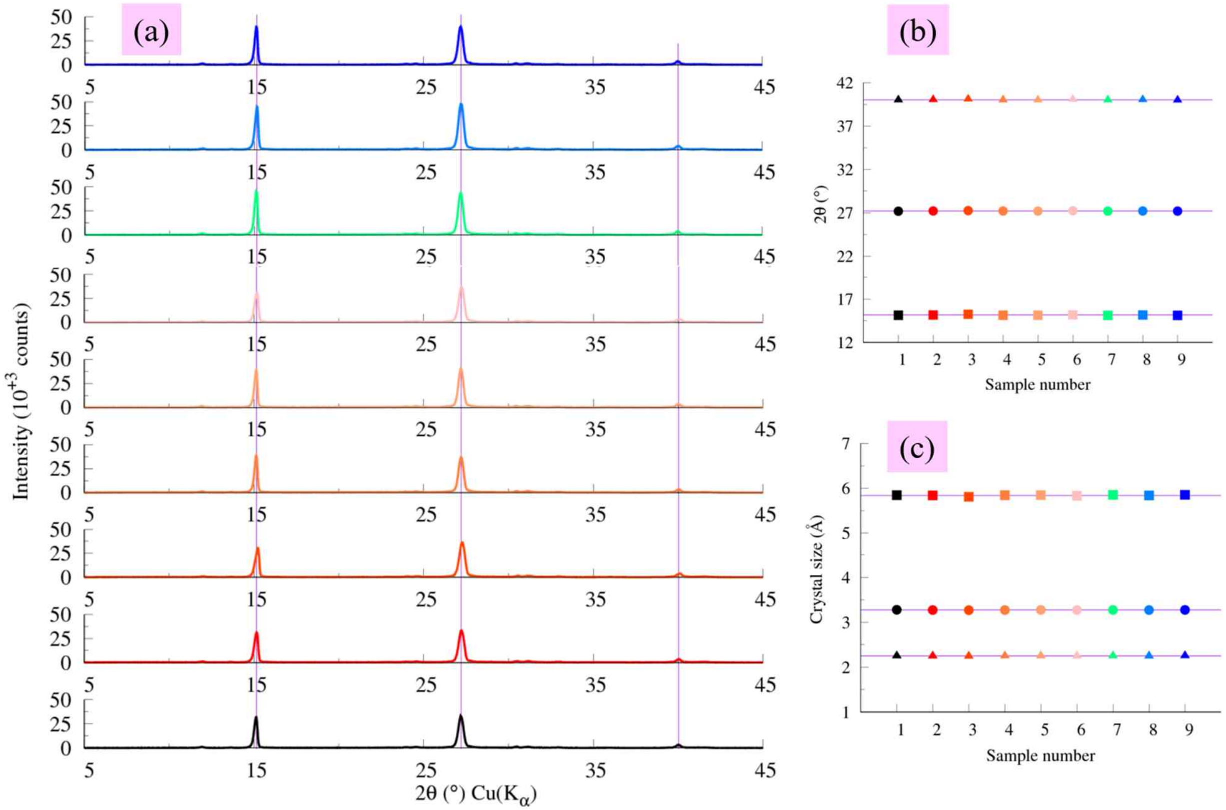

Figure 3: (a) Results of the PXRD analysis for the (—) 2-ATA as such and the 2-ATA excess undissolved solids in the suspension (after drying) with solvents (—) methanol, (—) ethanol, (—) 1-propanol, (—) 1-butanol, (—) 2-propanol, (—) 2-butanol, (—) 2-methyl-2-propanol, and (—) 3-methyl-1-butanol. (b) 2θ values for the peaks with P/N (peak-to-noise) ratio, higher than 20%. (c) Crystal size, calculated using the Scherrer relation [10], based on the 2θ values from part (b).

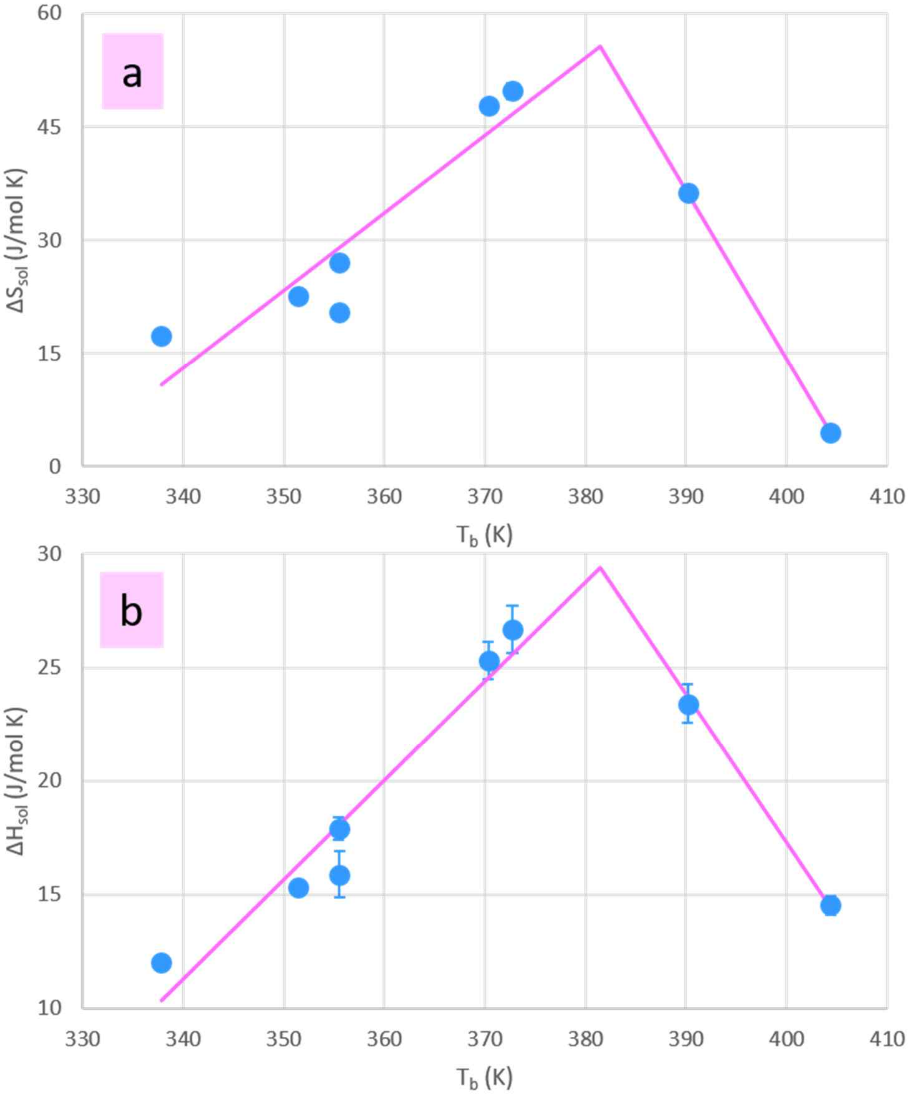

Figure 4: (a) ΔS_{sol} and (b) ΔH_{sol} versus boiling temperature of the used alcoholic solvents, T_b. (●) Values, based on the estimates for A and B, reported in Table 3, with confidence intervals serving as corresponding error bars and (—) optimized polygonal line with 2 segments.

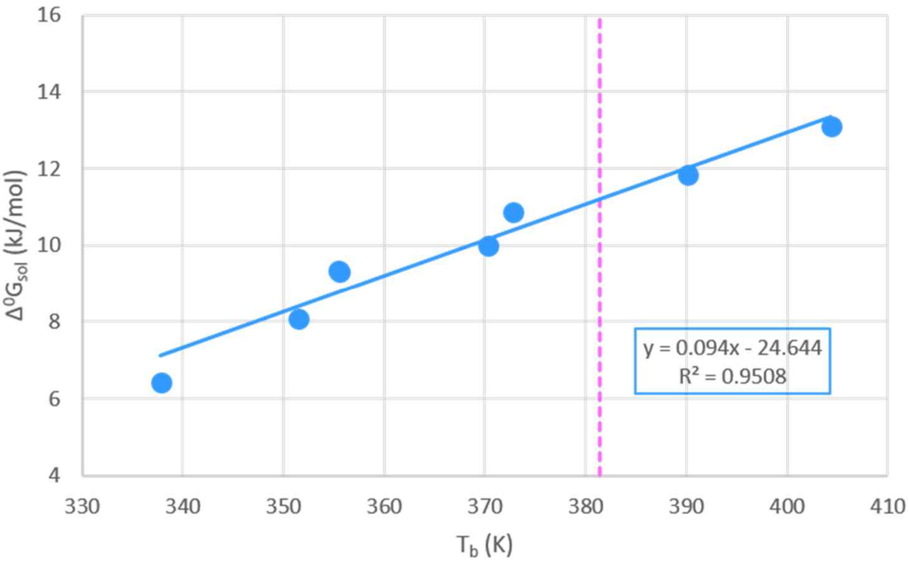

Figure 5: (●) Δ^0G_{sol}, obtained via Eq. (21) and reported in Table 6, versus boiling temperature of the used alcoholic solvents, T_b. (—) linear trendline and dashed line represents T* = 381.1 K.

Table 1: Detailed information of the solute and solvents used. The mass fraction purity of each material was provided by the suppliers.

Materials	CAS	Molecular formula	Source	Mass fraction purity	Purification methods
2-aminoterephthalic acid	10312-55-7	$C_8H_7NO_4$	Sigma-Aldrich, USA	0.990	None
methanol	67-56-1	CH_4O	Daejung Chemicals & Metals Co., Ltd., Korea	> 0.998 (a)	None
ethanol	64-17-5	C_2H_6O	Daejung Chemicals & Metals Co., Ltd., Korea	> 0.999	None
1-propanol	71-23-8	C_3H_8O	Daejung Chemicals & Metals Co., Ltd., Korea	> 0.995	None
1-butanol	71-36-3	$C_4H_{10}O$	Daejung Chemicals & Metals Co., Ltd., Korea	> 0.990	None
2-propanol	67-63-0	C_3H_8O	Sigma-Aldrich, USA	0.995	None
2-butanol	78-92-2	$C_4H_{10}O$	Sigma-Aldrich, USA	0.990 (b)	None
2-methyl-2-propanol	75-65-0	$C_4H_{10}O$	Daejung Chemicals & Metals Co., Ltd., Korea	> 0.995	None
3-methyl-1-butanol	123-51-3	$C_5H_{12}O$	Daejung Chemicals & Metals Co., Ltd., Korea	> 0.980	None
fumaric acid	110-17-8	$C_4H_4O_4$	Carl Roth GmbH	0.995	None
benzoic acid	65-85-0	$C_7H_6O_2$	Sigma-Aldrich, USA	> 0.995	None
water	7732-18-5	H_2O	Daejung Chemicals & Metals Co., Ltd., Korea	≥ 0.999 (c)	None

(a) '>' signifies the product specification 'above certain purity', provided by the manufacturer. (b) Racemic mixture. (c) HPLC grade.

Table 2: Experimental ($x_1 = x^{exp}$) and calculated mole fraction solubility of crystalline 2-aminoterephthalic acid in alcoholic solvents at the temperature range from 303.15 K to 338.15 K. The standard uncertainty of T is u (T) = 0.1 K and the average experimental pressure was 0.1021 MPa with standard uncertainty u (P) = 0.0006 MPa [53]. The relative standard uncertainty of the molar solubility is u_r (x^{exp}) = 0.054.

T/K	x^{exp}	$x^{Van't Hoff}$	$x^{\lambda h}$
methanol			
303.15	0.06848	0.06824	0.06857
313.15	0.07935	0.07948	0.07942
318.15	0.08525	0.08547	0.08529
323.15	0.09172	0.09171	0.09149
328.15	0.09818	0.09819	0.09802
333.15	0.10493	0.10491	0.10491
338.15	0.11196	0.11187	0.11218
ethanol			
303.15	0.03492	0.03478	0.03493
308.15	0.03833	0.03839	0.03844
313.15	0.04219	0.04225	0.04220
318.15	0.04610	0.04635	0.04624
323.15	0.05105	0.05070	0.05058
328.15	0.05516	0.05530	0.05520
333.15	0.05996	0.06017	0.06016
338.15	0.06549	0.06531	0.06547

1-propanol			
303.25	0.01367	0.01377	0.01379
308.75	0.01655	0.01647	0.01648
313.75	0.01933	0.01928	0.01928
318.15	0.02233	0.02204	0.02204
323.15	0.02556	0.02556	0.02555
328.15	0.02932	0.02951	0.02950
333.15	0.03342	0.03392	0.03392
338.15	0.03924	0.03883	0.03885
1-butanol			
303.15	0.00721	0.00733	0.00735
308.15	0.00854	0.00851	0.00852
313.15	0.00980	0.00983	0.00983
318.15	0.01125	0.01131	0.01129
323.15	0.01314	0.01295	0.01293
333.15	0.01684	0.01678	0.01679
338.15	0.01888	0.01898	0.01904
2-propanol			
303.15	0.02115	0.02103	0.02111
308.15	0.02361	0.02362	0.02364
318.15	0.02933	0.02945	0.02938
323.15	0.03265	0.03271	0.03262
338.15	0.04409	0.04403	0.04409
2-butanol			
303.15	0.00989	0.00995	0.00996

308.15	0.01187	0.01181	0.01181
313.15	0.01386	0.01394	0.01393
323.15	0.01925	0.01912	0.01911
328.15	0.02217	0.02225	0.02223
338.15	0.02970	0.02969	0.02971
2-methyl-2-propanol			
303.15	0.02164	0.02159	0.02171
308.15	0.02370	0.02393	0.02397
313.15	0.02684	0.02643	0.02640
318.15	0.02933	0.02909	0.02903
323.15	0.03150	0.03194	0.03185
328.15	0.03506	0.03496	0.03489
333.15	0.03754	0.03816	0.03815
338.15	0.04206	0.04155	0.04167
3-methyl-1-butanol			
303.15	0.00536	0.00534	0.00537
308.15	0.00583	0.00586	0.00587
313.15	0.00643	0.00642	0.00640
323.15	0.00764	0.00763	0.00759
333.15	0.00895	0.00898	0.00897
338.15	0.00972	0.00970	0.00973

Table 3: Correlated parameters with confidence interval for the Van't Hoff model for crystalline 2-aminoterephthalic acid in alcoholic solvents. RMSD and RAD are obtained via Eqs. (13) and (14), respectively.

Solvent	A	B	RMSD	RAD (%)
methanol	2.093 ± 0.065	-1448.3 ± 21.1	$1.38\ 10^{-4}$	0.128
ethanol	2.724 ± 0.178	-1846.9 ± 57.1	$1.97\ 10^{-4}$	0.349
1-propanol	5.759 ± 0.515	-3046.0 ± 166.4	$2.63\ 10^{-4}$	0.750
1-butanol	4.286 ± 0.320	-2789.7 ± 104.4	$1.00\ 10^{-4}$	0.737
2-propanol	3.280 ± 0.165	-2165.1 ± 53.5	$8.26\ 10^{-5}$	0.258
2-butanol	5.963 ± 0.200	-3205.5 ± 65.4	$7.43\ 10^{-5}$	0.428
2-methyl-2-propanol	2.489 ± 0.545	-1917.2 ± 175.0	$3.77\ 10^{-4}$	1.010
3-methyl-1-butanol	0.539 ± 0.134	-1749.1 ± 43.6	$2.22\ 10^{-5}$	0.301

Table 4: Correlated parameters with confidence interval for the λh model for crystalline 2-aminoterephthalic acid in alcoholic solvents. RMSD and RAD are obtained via Eqs. (13) and (14), respectively.

Solvent	λ	h	RMSD	RAD (%)
methanol	0.258 ± 0.067	4458.8 ± 21.8	$1.43\ 10^{-4}$	0.129
ethanol	0.267 ± 0.174	6081.9 ± 56.8	$1.96\ 10^{-4}$	0.252
1-propanol	0.705 ± 0.508	4274.2 ± 164.1	$2.59\ 10^{-4}$	0.750
1-butanol	0.241 ± 0.367	11141.5 ± 119.8	$1.15\ 10^{-4}$	0.795
2-propanol	0.270 ± 0.060	7370.2 ± 19.5	$3.02\ 10^{-5}$	0.101
2-butanol	0.625 ± 0.206	5065.5 ± 67.4	$7.65\ 10^{-5}$	0.448
2-methyl-2-propanol	0.176 ± 0.052	9530.0 ± 168.3	$3.62\ 10^{-4}$	1.036
3-methyl-1-butanol	0.028 ± 0.017	49942.1 ± 55.6	$2.83\ 10^{-5}$	0.358

Table 5: Solvatochromic parameters (α, β and π*) and Hildebrand solubility parameter (δ_H) for the pure alcoholic solvents. The former are obtained from Marcus [34] and the latter is calculated according to Fedors [22, 54].

Solvent	α	β	π*	$\sqrt{\delta_H}$
methanol	0.98	0.66	0.6	28.1609
ethanol	0.86	0.75	0.54	25.7225
1-propanol	0.84	0.90	0.52	24.2105
1-butanol	0.84	0.84	0.47	23.1760
2-propanol	0.76	0.84	0.48	20.9536
2-butanol	0.69	0.80	0.40	20.4118
2-methyl-2-propanol	0.42	0.93	0.41	19.9219
3-methyl-1-butanol	0.84	0.86	0.40	22.0295

Table 6: Results for the Van't Hoff analysis regarding the solubility of crystalline 2-aminoterephthalic acid in alcoholic solvents. Standard deviations for Δ^0G_{sol}, Δ^0H_{sol} and Δ^0S_{sol} are obtained from linear regression and the standard deviations for ζ_H and ζ_{TS} is obtained by Eqs. (S-22) and (S-25), see section S.9 in the Supplementary Content.

Solvent	Δ^0G_{sol} (kJ mol^{-1})	Δ^0H_{sol} (kJ mol^{-1})	Δ^0S_{sol} (J mol^{-1} K^{-1})	ζ_H (-)	ζ_{TS} (-)
methanol	6.44 ± 0.01	12.0 ± 0.1	17.3 ± 0.1	0.683 ± 0.001	0.317 ± 0.001
ethanol	8.08 ± 0.01	15.3 ± 0.1	22.6 ± 0.1	0.679 ± 0.002	0.321 ± 0.002
1-propanol	9.98 ± 0.01	25.3 ±0.3	47.8 ± 0.3	0.623 ± 0.003	0.377 ± 0.003
1-butanol	11.8 ± 0.01	23.4 ± 0.3	36.3 ± 0.3	0.669 ± 0.003	0.331 ± 0.003
2-propanol	9.34 ± 0.01	17.9 ± 0.1	27.0 ± 0.1	0.676 ± 0.002	0.324 ± 0.002
2-butanol	10.9 ± 0.01	26.7 ± 0.2	49.7 ± 0.2	0.628 ± 0.002	0.372 ± 0.002
2-methyl-2-propanol	9.31 ± 0.01	15.9 ± 0.3	20.5 ± 0.3	0.707 ± 0.006	0.293 ± 0.006
3-methyl-1-butanol	13.1 ± 0.01	14.5 ± 0.1	4.4 ± 0.1	0.911 ± 0002	0.089 ± 0.002